

## EXPERIMENTAL STUDY ON SURFACE MORPHOLOGY, DENSITY AND RELATIVE DIELECTRIC CONSTANT OF HIGH-DENSITY POLYETHYLENE (HDPE)/NATURAL RUBBER (NR) BIOCOMPOSITES

MOHD HARIS ASYRAF SHEE KANDAR<sup>1</sup>, NOR AKMAL MOHD JAMAIL<sup>1\*</sup>, SUSAMA BAGCHI<sup>1</sup>, NOR SHAHIDA MOHD JAMAIL<sup>2</sup>, RAHISHAM ABD RAHMAN<sup>1</sup>, QAMARUL EZANI KAMARUDIN<sup>3</sup>, FAHMIRUDDIN ESA<sup>4</sup> AND SANJOY KUMAR DEBNATH<sup>1</sup>

<sup>1</sup>Faculty of Electrical and Electronic Engineering, Universiti Tun Hussein Onn Malaysia (UTHM), 86400 Batu Pahat, Johor, Malaysia. <sup>2</sup>Department of Information System, Prince Sultan University (PSU), Riyadh Saudi Arabia. <sup>3</sup>Faculty of Mechanical and Manufacturing Engineering, Universiti Tun Hussein Onn Malaysia (UTHM), 86400 Batu Pahat, Johor, Malaysia. <sup>4</sup>Faculty of Applied Sciences and Technology, Universiti Tun Hussein Onn Malaysia (UTHM), 86400 Batu Pahat, Johor, Malaysia.

\*Corresponding author: norakmal@uthm.edu.my

Submitted final draft: 29 August 2021

Accepted: 24 February 2022

<http://doi.org/10.46754/jssm.2022.4.017>

**Abstract:** This study examines the surface morphology, density and relative dielectric constant of three formulations of HDPE/NR prior to further development of HDPE/NR/Empty Fruit Bunch (EFB), HDPE/NR/Pineapple Leaf (PAL) and HDPE/NR/Coconut Coir (CC). The used weight percentages of the EFB, PAL and CC fillers in this study were 10 wt. %, 20 wt. % and 30 wt. %. HDPE/NR/EFB, HDPE/NR/PAL and HDPE/NR/CC were prepared using a two-rotor mill blending method. It is known that the presence of bio-composite filler in base can affect the density, relative dielectric constant (permittivity) and as well as the surface morphology. This study also found that the PAL filler had about 12% lower density at 20 wt. % compared with EFB and CC fillers of the same weight percentage. In contrast to PAL and CC fillers, the EFB filler had a lower relative dielectric constant of about 8.7% at 4.5 Hz. Future work can focus on enhancing the production of a lower space charge accumulation.

Keywords: Density, FESEM, HDPE, permittivity.

### Introduction

HDPE, a semi-crystalline is widely used as a commodity thermoplastic in various applications, such as polymeric insulation. Singh and Vimal (2016) reported that HDPE is low-cost and has good bio-compatibility, chemical resistance, recyclability, higher flexibility and impact, processability and very good electrical, mechanical, thermal and physical properties. However, HDPE has drawbacks such as low resilience and elasticity. Mixing HDPE with NR is the only way to resolve its restriction, in order to compensate for HDPE's weakness. This is because NR is highly elastic (He & Gao, 2017) and mechanically strong, low heat build-up and flexible but NR has significant drawbacks in application, such as intolerance to oil-based substances, is hard to press and unstable at high temperature. NR can be improved to meet application requirements by adding a filler. Homogenous dispersion of bio-composites in

polymer matrix has always been a challenge. To resolve the weak adhesion matrix between base and filler, an investigation was done by controlling the wt. % of fillers and incorporating various bio-composite fillers into base matrix (Jojibabu & Zhang, 2020). Natural fibers offer many advantages compared to inorganic fibers. Due to its low cost, lower density, high specific strength, biodegradability, renewable nature, harmlessness to humans and less abrasive to processing equipment, EFB has been selected and could lead to significant improvements in dielectric properties (Mahmud *et al.*, 2017) compared to neat polymer. While PALF is low density, low cost, nano abrasive, low energy consumption, high specific properties, biodegradable, good in dielectric constant, has specific strength and stiffness and excellent potential reinforcement (Asim *et al.*, 2015) in composite matrices. CC was also investigated due to its low cost, extensive use in fiber-

reinforced polymer composite, good dielectric constant, light weight and excellent mechanical and electrical properties (Khan & Joshi, 2014). In this study, EFB, PAL and CC were used as fibres. These three bio-composite fillers were investigated by varying the weight percentage (wt. %), e.g., 10 wt. %, 20 wt. % and 30 wt. %. The density kit instrument, field emission scanning electron microscope and dielectric test fixture were used to study the characteristics of each species. Also, the interfacial adhesion of bio-composite fillers was characterized using the field emission scanning electron microscope (Nimanpure & Hashmi, 2018). The morphology of fractured surface, density of the test specimen and relative dielectric constant (permittivity) of test material were determined as well.

## Experimental Arrangement

### Materials

High-density polyethylene and standard Malaysian rubber (SMR) grade 10 were used as a bio-composite base. Lotte Chemical Titan Holding Berhad, Malaysia, supplied HDPE pellets with a density and melting temperature of 0.89 g/cm<sup>3</sup> and 125°C to 135°C respectively. SMR 10 was obtained from Seng Hin Rubber (M) Sdn. Bhd., Malaysia with a density of 0.88 g/cm<sup>3</sup>. The melting temperature for SMR 10 is between 28°C and 40°C.

### Preparation of HDPE/NR-based Bio-composites

The detailed formulation of HDPE/NR-based bio-composites is shown in Table 1. The selected weight percentage of the fillers is between 10 and 30 wt. %. This range was selected because of it is the most significant and suitable for biocomposites. Previous research (Khashab *et al.*, 2014) found that below 10 wt. % is normally used for plastic granulator machine nanofillers. The bio-composite filler consists of an empty fruit bunch (EFB), a pineapple leaf (PAL) and a coconut coir (CC) fiber. First, EFB, PAL and CC fibers were dried in a high-capacity oven (Hihat *et al.*, 2017) for one day at 60°C to remove water that could be trapped in a bio-composite filler. These fibers were crushed prior to extrusion. The Fritsch rotor mill machine (Liu *et al.*, 2021) was used to mill these fibers into a particle size of 150 µm. After that a mixture of approximately 200 g containing all HDPE pellets, SMR 10 and bio-composite fillers was compounded on a two-rotor mill machine (Drobny, 2014) at a speed of 7 Hz maintaining the temperature at 193°C. All these HDPE/NR-based bio-composites were again crushed for a second time using a plastic granulator machine before the compression process. Finally, in order to produce a square prism shape with a dimension of 24.0 cm x 24.0 cm x 0.3 cm (depending on the size of the mould), the pre-heating time, press time and temperature of the compression moulding machine (Shamsuri, 2015) were set at 20 minutes, 3 tone

Table 1: Composition of the HDPE/NR-based bio-composites

Samples	Group	Content Filler Weight Percentages (wt. %)
HDPE+NR+EFB10	E1	10
HDPE+NR+EFB20	E2	20
HDPE+NR+EFB30	E3	30
HDPE+NR+PAL10	P1	10
HDPE+NR+PAL20	P2	20
HDPE+NR+PAL30	P3	30
HDPE+NR+CC10	C1	10
HDPE+NR+CC20	C2	20
HDPE+NR+CC30	C3	30

presses at 20 minutes and 170°C, respectively. To ensure that the mass volume was sufficient for compression moulding, an additional 10% of the mass sample was required. Overall process and analysis of new Polymer Bio-composite configuration is shown in Figure 1.

**Field Emission Scanning Electron Microscope (FESEM)**

FESEM model JEOL JSM-7600F was used in this study to investigate the inter-relationships between the HDPE, NR grade SMR 10, EFB, PAL and CC fibers, i.e. the interaction between the filler and the polymer matrix. The size of the specimens for the FESEM is 1 cm x 1 cm (square shape). The specimens were coated using 30 mA of gold (Au) for 40 seconds. Copper tape was used as a sample holder for FESEM. This method was presented by Kamarulzaman *et al.*

(2014). Morphology of the surface composite was also analyzed and observed by FESEM at room temperature. The sample was considered perpendicular to the fractured surface.

**Density Kit**

The density kit instrument is crafted by Mettler Toledo which is modelled XS64 with maximum 61 g and d = 0.1 mg. The main density test apparatus is the sample holder, clip, thermometer, beaker, distilled water, pan and basket. Before the density test, all the specimens were gone through a Carver Hydraulic Press to form a flat circle shape to avoid the scattering of the filler completely. As it was expected, the temperature affected the density of the water. The density can be measured by using the formula given below (Hopkins, 2013).

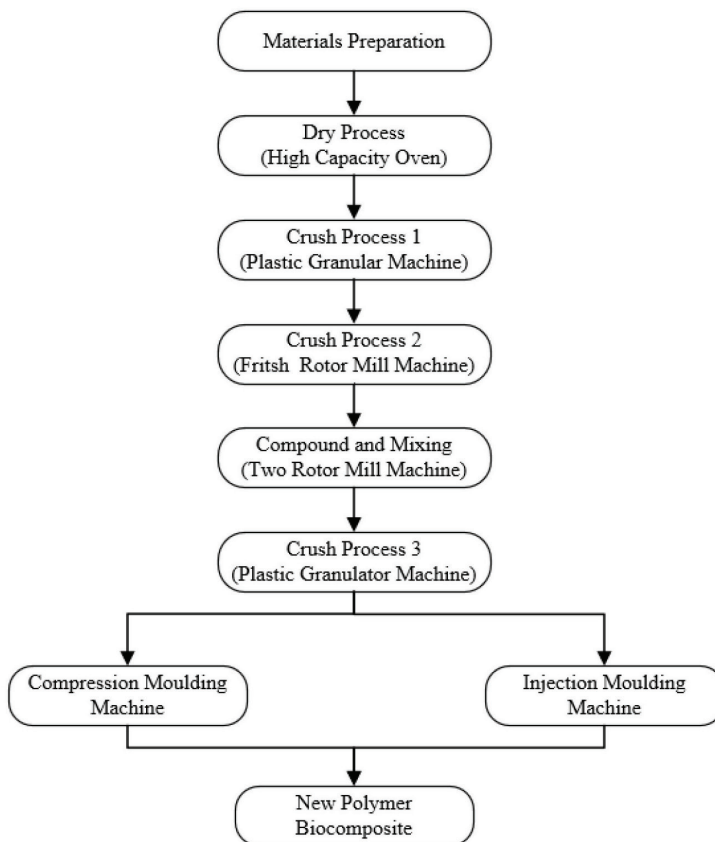


Figure 1: Overall process and analysis of new Polymer Biocomposite configuration

$$\rho = m/V \tag{1}$$

where,

- $\rho$  - density of sample [g.cm<sup>-3</sup>]
- $m$  - mass of sample [g]
- $V$  - volume of mould [cm<sup>3</sup>]

**Dielectric Test Fixture**

Keysight 16451B dielectric test fixture was used to analyze the relative dielectric constant (permittivity) of the test material and it was manufactured by Keysight Technologies. Its frequency range and applicable voltage range were ≤30 MHz and ±42 V peak max (AC+DC). The used cable length (setting) and the operating temperature were around 1 m and 0°C to 55°C respectively. The operating humidity was ≤95 % (40°C) and the weight was 3.7 kg, including accessories. The voltage and current were adjusted to 800 mV and 18 mA (ranging from 0.01 A to 20 mA) for experimental purposes. This dielectric test fixture read up to 201 data points and the start frequency was set at 40 Hz and the end frequency was set at 1 MHz. Table 2 illustrates three methods of measurement that

are contacting electrode method (rigid metal electrode), contacting electrode method (thin film electrode) and non-contacting electrode method (air gap method). For this experimental setup, contacting electrode method was used with rigid metal electrode because the specimens were of thick material having flat surface.

The dielectric constant (permittivity) can be determined using the following formula (Markell, 2016).

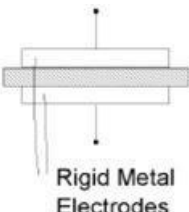
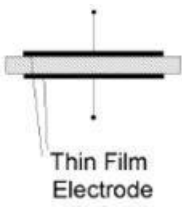
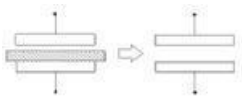
$$\epsilon = \epsilon_0 \epsilon_r \tag{1}$$

$$\epsilon = \frac{t}{A} C_p \tag{2}$$

where,

- $\epsilon$  - Dielectric constant (permittivity) [F/m]
- $\epsilon_0$  - Space permittivity = 8.854x10<sup>-12</sup> [F/m]
- $\epsilon_r$  - Relative dielectric constant (Relative permittivity) of test material
- $t$  - Average thickness of test material [m]
- $A$  - Area of Guarded electrode [m<sup>2</sup>]
- $C_p$  - Equivalent parallel capacitance [F]
- $d$  - Diameter of electrode [m]

Table 2: Measurement method presented by dielectric test fixture

Measurement Method	Contacting Electrode Method (used with Rigid Metal Electrode)	Contacting Electrode Method (used with Thin Film Electrode)	Non-contacting Electrode Method (Air Gap Method)
Electrode Structure			
Operation	Simple	Medium	Complex
Applicable Test Material	<ul style="list-style-type: none"> <li>• Thick material</li> <li>• Smooth material</li> </ul>	Materials on which thin film electrode can be applied without changing its characteristics	<ul style="list-style-type: none"> <li>• Including contacting method's applicable test materials</li> <li>• Highly compressible material</li> <li>• Soft material</li> </ul>
Electrodes of 16451B	Electrode-A Electrode-B	Electrode-C Electrode-D	Electrode-A Electrode-B

Consequently, the relative permittivity (relative dielectric constant) of test samples,  $\epsilon_r$ , can also be calculated by calculating the capacitance value by using the following equation.

$$\epsilon_r = \frac{t \times C_p}{A \times \epsilon_0} \tag{3}$$

$$\epsilon_r = \frac{t \times C_p}{\pi \times \left(\frac{d}{2}\right)^2 \times \epsilon_0} \tag{4}$$

## Experimental Results

### Morphology of the Samples

Figure 2 shows the FESEM micrographs of the fractured surface of HDPE/NR with and without 10 - 30 wt. % fillers, respectively. Interaction between SMR 10 and HDPE had lesser agglomeration (Piah & Darus, 2003) and matte texture surface because HDPE/NR bio-composite with a medium and low filler content is homogenously dispersed (Piah & Darus, 2003) as exposed in Figure 2 (a), 2 (b) and 2 (c). Therefore, the interaction of HDPE/NR without fillers is strong as shown in Figure 2 (j).

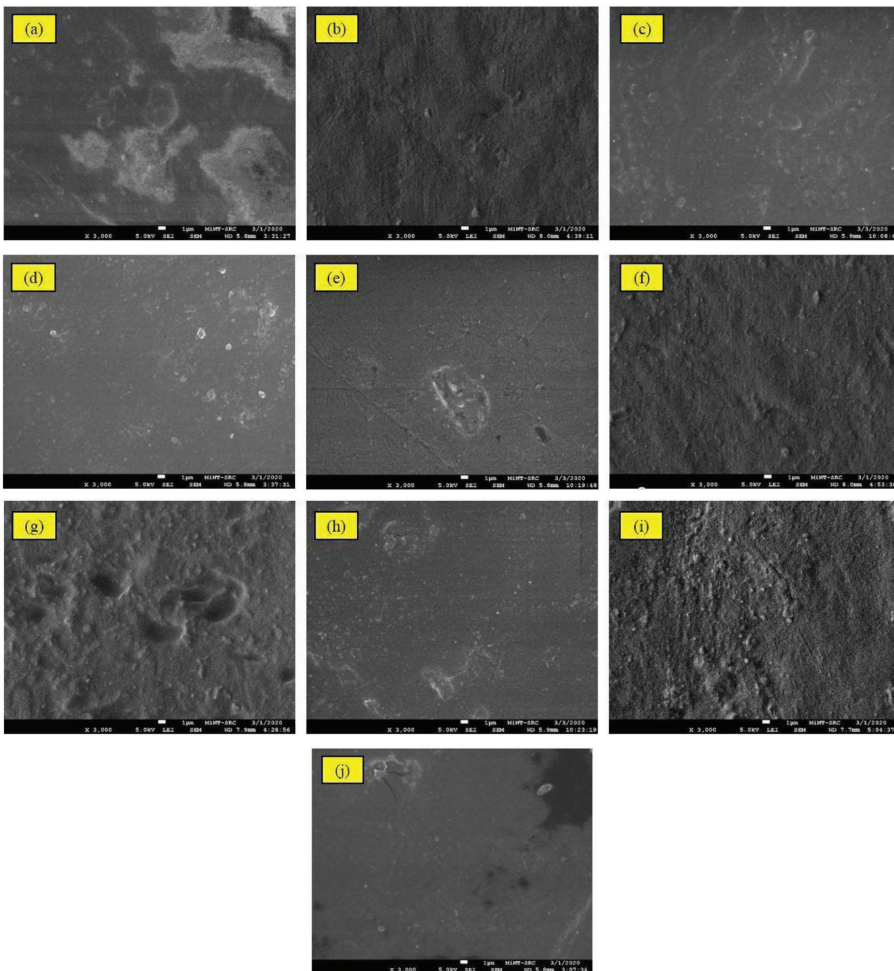
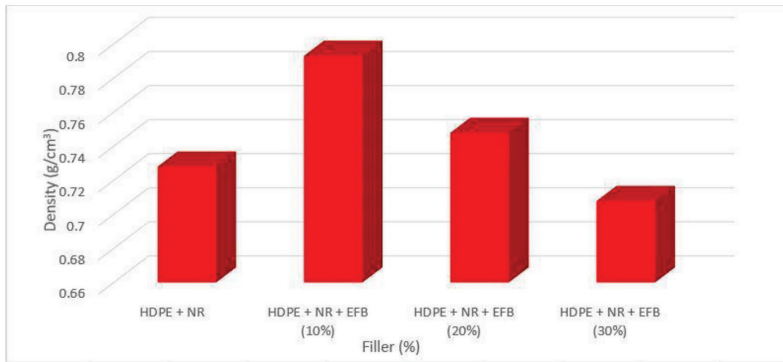


Figure 2: FESEM images of test material of HDPE/NR (a) HDPE+NR+EFB 10%, (b) HDPE+NR+PAL 10%, (c) HDPE+NR+CC 10%, (d) HDPE+NR+EFB 20%, (e) HDPE+NR+ PAL 20%, (f) HDPE+NR+CC 20%, (g) HDPE+NR+EFB 30%, (h) HDPE+NR+PAL 30%, (i) HDPE+NR+CC 30%, (j) HDPE+NR

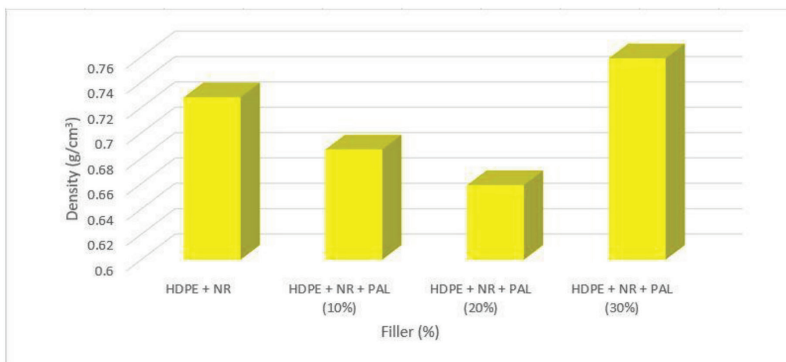
On the contrary, medium agglomerate was formed in Figure 2 (d), 2 (e) and 2 (f) compared to earlier cases as shown in Figure 2 (a), 2 (b) and 2 (c) due to 20 wt. % of bio-composite fillers, i.e. higher content of bio-composite fillers. As a result, the fractured surface of the material compounding became rough (Prusty & Barik, 2018; Kumar & Sharma, 2018). It can be seen from the Figure 2 (g) and 2 (i) that the size of the composition is larger than what was seen in 2 (h). These samples are larger due to the 30 wt. % of bio-composite fillers and the high agglomerates (Prasad, 2018) are observed in both composite samples. On the other hand, highly rough surface was obtained and compared to Figures 2 (a), 2 (b), 2 (c), 2 (d), 2 (e), 2 (f) and 2 (i) during the compound process due to the higher level of bio-composite filler for which the polymer matrix was unable to disperse uniformly. Hence, the adhesion matrix between the base and the fiber had poor compatibility and was not sufficient.

**Density of the Samples**

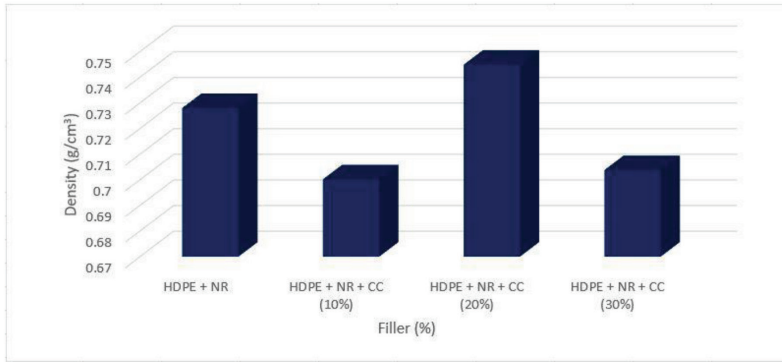
Based on the experimental data, the samples were tested three times in order to obtain an average density reading. The resulting density of HDPE+NR+EFB, HDPE+NR+PAL and HDPE+NR+CC are shown in Figure 3. The density for 10 wt. % of the EFB filler was higher (0.7930 g/cm<sup>3</sup>) than that with 20 wt. % and 30 wt. %. While the density obtained without filler (0.728 g/cm<sup>3</sup>) was lower than both 10 wt. % and 20 wt. % of EFB fillers. Goll and Venzon (2018) found that the higher filler level resulted in lower density value of the sample. Perpendicular to EFB, PAL fiber had high specific properties and had specific strength and stiffness (Senawi & Salleh, 2012). Higher content of filler gives higher density value of the test sample and was reported in Linec and Mušič (2019). The density for 30 wt. % of PAL filler was greater than 10 wt. % and 20 wt. % of PAL filler, which is 0.7588 g/cm<sup>3</sup>. Besides, the density for 10 wt. % (0.7002 g/cm<sup>3</sup>) of CC filler was less than 20



(a)



(b)



(c)

Figure 3: Density of (a) HDPE+NR+EFB, (b) HDPE+NR+PAL, (c) HDPE+NR+CC

wt. % of CC filler and without filler. This shows that the same concept can be applied to the EFB, where the level of weight percentage (Goll & Venzon, 2018) affects the density value. In other words, the density value decreased when the wt. % of filler increased, due to the lighter density of filler material and void content. This is due to the imbalance of filler and matrix weight percentage. On the whole, HDPE+NR+CC may be considered to have inferior density compared to HDPE+NR+EFB and HDPE+NR+PAL because CC fiber is light in weight (Asasutjarit & Hirunlabh, 2007) and has a good dielectric constant (permittivity) that can give excellent mechanical and electrical performance (Kandar, 2019; 2020).

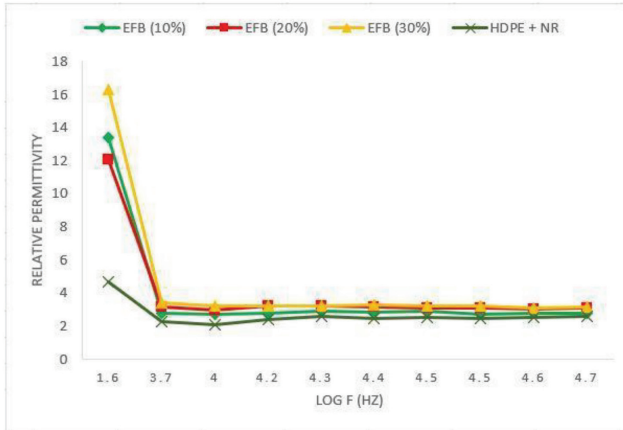
**Relative Dielectric Constant (Permittivity) of the Samples**

The dielectric test fixture reads up to 201 data points for relative dielectric constant outputs ranging from 40 Hz (start) to 1 MHz (end). The permittivity value of the 201 data points is strikingly similar. So, the best (10 data points near 40 Hz were selected – where permittivity values start to be strikingly similar or saturated) 1 to 10 datapoints were plotted. Table 3 shows the frequency and Figure 4 displays the relative dielectric constant with and without filler. The relative permittivity value for EFB (30%) filler was higher than that for EFB (10%), EFB (20%) and without filler, which is 3.17 at

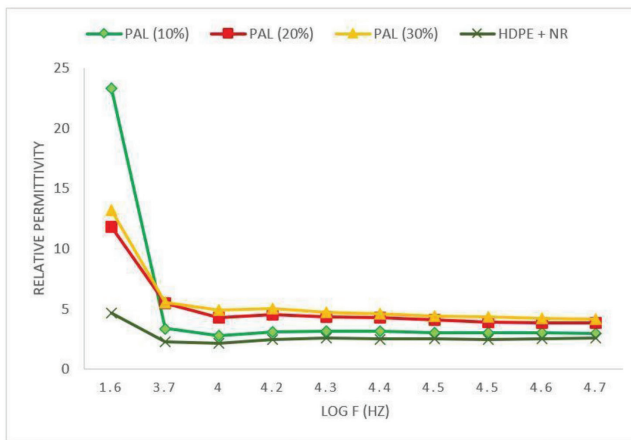
4.7 Hz. Zhong and Long (2020) reported that continuous addition of filler might increase the permittivity value at room temperature. Further, the relative permittivity value for PAL (10%) filler was inferior to that of PAL (20%) and PAL (30%), which was 3.16 compared to 4.27 and 4.57 at 4.4 Hz. Results published by Wang (2020) considered filler content of aluminum, where low level of filler content of Al decreased the permittivity value. The relative permittivity value for CC (30%) filler was bigger than that for CC (10%) and CC (20%) which was 4.54 compared to 3.11 and 4.15 at 4 Hz and the same principle that Zhong and Long (2020) reported was observed. To sum up, the relative dielectric constant (permittivity) value is higher for each filler, between 1.6 Hz to 3.7 Hz. This is because there is greater fluctuation due to the

Table 3: Frequency

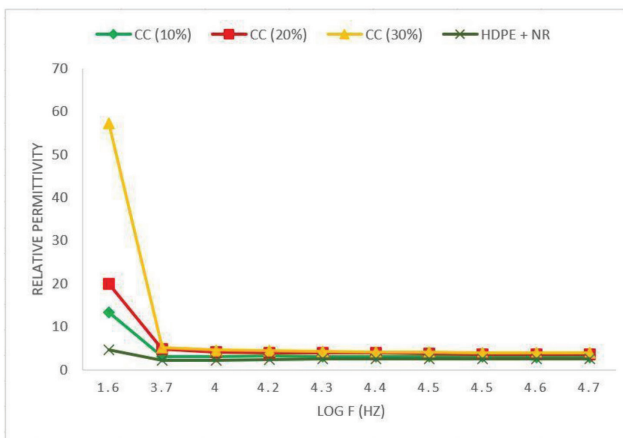
Frequency (Hz)	Log F (Hz)
40.00	1.60
5039.00	3.70
10039.00	4.00
15039.00	4.20
20039.00	4.30
25039.00	4.40
30038.00	4.50
35038.00	4.50
40038.00	4.60
45038.00	4.70



(a)



(b)



(c)

Figure 4: Relative Dielectric Constant (Permittivity) of (a) HDPE+NR+EFB, (b) HDPE+NR+PAL, (c) HDPE+NR+CC



low frequency and it vacillates between 3.7 Hz to 4.7 Hz slowly due to the high frequency (Yadav & Sahu, 2010). In short, when the filler content rises, the permittivity increases.

## Conclusion

This study reveals that the PAL filler has an inferior density compared to EFB and CC filler due to the nano abrasive, high specific properties, good dielectric constant, specific strength and stiffness and excellent potential reinforcement in composite matrices. Unquestionably, the relative dielectric constant of the EFB filler for 10 wt. %, 20 wt. % and 30 wt. % can be highlighted as the best due to its lower permittivity values compared to PAL and CC fillers and could lead to significant improvements in dielectric properties compared to neat polymer. If the bio-composites filler with a low wt. % is seen through a field emission scanning electron microscope, less void, agglomerated, matte texture surface, homogenously dispersed and good adhesion matrix between base and matrix compatibility can be observed. Future research can focus on enhancing the production of a lower space charge.

## Acknowledgements

The authors gratefully acknowledge the Ministry of Higher Education Malaysia for supporting this research under Fundamental Research Grant Scheme for Research Acculturation of Early Career Researchers (FRGS-RACER) Vot No. RACER/1/2019/TK04/UTHM//6, Universiti Tun Hussein Onn Malaysia and Prince Sultan University, Saudi Arabia for technical support.

## References

Asasutjarit, C., Hirunlabh, J., Khedari, J., Charoenvai, S., Zeghamati, B., & Shin, U. C. (2007). Development of coconut coir-based lightweight cement board. *Construction and Building Materials*, 21(2), 277-288. <https://doi.org/10.1016/j.conbuildmat.2005.08.028>

- Asim, M., Abdan, K., Jawaid, M., Nasir, M., Dashtizadeh, Z., Ishak, M. R., & Hoque, M. E. (2015). A review on pineapple leaves fibre and its composites. *International Journal of Polymer Science*, 2015, 1-16. <http://dx.doi.org/10.1155/2015/950567>
- Drobny, J. G. (2014). Processing methods applicable to Thermoplastic Elastomers. In *Handbook of Thermoplastic Elastomers*. <https://doi.org/10.1016/b978-0-323-22136-8.00004-1>
- Goll, M. F. G. H., Venzon, J. S., Vegini, A. A., Eleotério, J. R., & Tavares, L. B. B. (2018). Composites based on low-density polyethylene combined with PET-coated sbs paperboard shavings. *Revista Materia*, 23(4). <https://doi.org/10.1590/s1517-707620180004.0582>
- He, Y., Gao, J., Gong, X., & Xu, J. (2017). The role of carbon nanotubes in promoting the properties of carbon black-filled natural rubber/butadiene rubber composites. *Results in Physics*, 7, 4352-4358. <https://doi.org/10.1016/j.rinp.2017.09.044>
- Hihat, S., Remini, H., & Madani, K. (2017). Effect of oven and microwave drying on phenolic compounds and antioxidant capacity of coriander leaves. *International Food Research Journal*, 24(2), 503-509. [http://www.ifrj.upm.edu.my/24%20\(02\)%202017/\(5\).pdf](http://www.ifrj.upm.edu.my/24%20(02)%202017/(5).pdf)
- Hopkins, P. F. (2013). A model for (non-lognormal) density distributions in isothermal turbulence. *Monthly Notices of the Royal Astronomical Society*, 430(3), 1880-1891. <https://doi.org/10.1093/mnras/stt010>
- Jojibabu, P., Zhang, Y. X., & Prusty, B. G. (2020). A review of research advances in epoxy-based nanocomposites as adhesive materials. *International Journal of Adhesion and Adhesives*, 96, 102454. <https://doi.org/10.1016/j.ijadhadh.2019.102454>
- Kamarulzaman, M. S., Muhamad, N. A., Jamail, N. A. M., Piah, M. A. M., Sidek,

- M. A. B., & Kasri, N. F. (2014). Moisture Absorption Analysis of Linear-Low-Density-Polyethylene Natural-Rubber Nanocomposite for HV Insulation. *Proceeding of the Electrical Engineering Computer Science and Informatics*, 1(1). <https://doi.org/10.11591/eecsi.v1.423>
- Kandar, M. H. A. S. (2017). Space Charges Analysis on XLPE Insulator with effect of uniform layer contamination. *Telecommunication Computing Electronics and Control*, 17(4). <https://doi.org/10.12928/TELKOMNIKA.v17i4.12765>
- Kandar, M. H. A. S. (2020). Review of space charge measurement by pulsed electro-acoustic technique. *Indonesian Journal of Electrical and Computer Science*, 20(2). <http://doi.org/10.11591/ijeecs.v20.i2.pp%25p>
- Khan, A., & Joshi, S. (2014). Effect of chemical treatment on electrical properties of coir fibre reinforced epoxy composites. *Journal of Physics*, 534(2014), 2-6. <https://doi.org/10.1088/1742-6596/534/1/012023>
- Khashaba, U. A., Aljinaidi, A. A., & Hamed, M. A. (2014). Nanofillers modification of Epocast 50-A1/946 epoxy for bonded joints. *Chinese Journal of Aeronautics*, 27(5), 1288-1300. <https://doi.org/10.1016/j.cja.2014.08.007>
- Kumar, S., & Sharma, R. (2018). Chip-to-Chip copper interconnects with rough surfaces: Analytical Models for parameter extraction and performance evaluation. *IEEE Transactions on Components, Packaging and Manufacturing Technology*, 8(2), 286-299. <https://doi.org/10.1109/TCPMT.2017.2774252>
- Liu, S. X., Chen, D., Plumier, B., Berhow, M., Xu, J., & Byars, J. A. (2021). Impact of particle size fractions on composition, antioxidant activities and functional properties of soybean hulls. *Journal of Food Measurement and Characterization*, 15(2), 1547-1562. <https://doi.org/10.1007/s11694-020-00746-0>
- Linec, M., & Mušič, B. (2019). The effects of silica-based fillers on the properties of epoxy molding compounds. *Materials*, 12(11), 1-11. <https://doi.org/10.3390/ma12111811>
- Mahmud, S. N. S., Jusoh, M. A., You, K. Y., Salim, N., Shaheen, S., & Sutjipto, A. G. E. (2017). Structural and dielectric properties of Polyurethane Palm Oil based filled empty fruit bunch. *International Journal of Advanced Engineering Research and Science*, 4(1), 259-264. <https://doi.org/10.22161/ijaers.4.1.42>
- Markell, J., Loop, S. S., Baker, E., Gu, G., Joseph, I., Lansdowne, C., ... Zhou, R. (2016). Calculating the relative permittivity constants of various dielectric materials using a parallel plate capacitor. *American Journal of Physics*, 73(1), 52-56. <https://doi.org/10.1016/j.ejca.2017.07.009>
- Nimanpure, S., Hashmi, S. A. R., Kumar, R., Nigrawal, A., & Naik, A. (2018). Electrical and dynamic mechanical analysis of sisal fibril reinforced epoxy composite. *IEEE Transactions on Dielectrics and Electrical Insulation*, 25(5), 2020-2028. <https://doi.org/10.1109/TDEI.2018.006661>
- Piah, M. A. M., Darus, A., & Hassan, A. (2003). Leakage current and surface discharge phenomena: Effect on tracking and morphological properties of LLDPE-natural rubber compounds. *Proceedings of the IEEE International Conference on Properties and Applications of Dielectric Materials*, 1, 347-350. <https://doi.org/10.1109/icpadm.2003.1218423>
- Prasad, M. S., Chen, R., Li, Y., Rekha, D., Li, D., Ni, H., & Sreedhar, N. Y. (2018). Polypyrrole Supported with Copper Nanoparticles Modified Alkali Anodized Steel Electrode for probing of glucose in real samples. *IEEE Sensors Journal*, 18(13), 5203-5212. <https://doi.org/10.1109/JSEN.2018.2829982>
- Prusty, K., Barik, S., & Swain, S. K. (2018). A correlation between the Graphene surface

- area, functional groups, defects and porosity on the performance of the nanocomposites. Functionalized Graphene nanocomposites and their derivatives: Synthesis, processing and applications. *Elsevier Inc*, 13, 265-283. <https://doi.org/10.1016/B978-0-12-814548-7.00013-1>
- Senawi, R., Salleh, R. M., Alauddin, S. M., Rashid, S. R. A., & Shueb, M. I. (2012). Effects of fiber loading and surface treatment on polylactic acid/empty fruit bunch fiber biocomposites. *CHUSER 2012 - 2012 IEEE Colloquium on Humanities, Science and Engineering Research*, 646-651. <https://doi.org/10.1109/CHUSER.2012.6504392>
- Shamsuri, A. A. (2015). Compression Moulding Technique for manufacturing biocomposite products. *International Journal of Applied Science and Technology*, 5(3), 23-26. [http://www.ijastnet.com/journals/Vol\\_5\\_No\\_3\\_June\\_2015/3.pdf](http://www.ijastnet.com/journals/Vol_5_No_3_June_2015/3.pdf)
- Singh, V. P., Vimal, K. K., Kapur, G. S., Sharma, S., & Choudhary, V. (2016). High-density polyethylene/halloysite nanocomposites: morphology and rheological behaviour under extensional and shear flow. *Journal of Polymer Research*, 23(3), 1-17. <https://doi.org/10.1007/s10965-016-0937-1>
- Wang, Z., Sun, K., Xie, P., Liu, Y., Gu, Q., & Fan, R. (2020). Permittivity transition from positive to negative in acrylic polyurethane-aluminum composites. *Composites Science and Technology*, 188, 107969. <https://doi.org/10.1016/j.compscitech.2019.107969>
- Yadav, V. S., Sahu, D. K., Singh, Y., & Dhukarya, D. C. (2010). The effect of frequency and temperature on dielectric properties of pure poly vinylidene fluoride (PVDF) thin films. *Proceedings of the International MultiConference of Engineers and Computer Scientists 2010, IMECS 2010*, 3, 1593-1596.
- Zhong, B., Long, Z., Yang, C., Li, Y., & Wei, X. (2020). Colossal dielectric permittivity in co-doping SrTiO<sub>3</sub> ceramics by Nb and Mg. *Ceramics International*, 46(12), 20565-20569. <https://doi.org/10.1016/j.ceramint.2020.05.174>